Formation of refractory black carbon by SP2-induced charring of organic aerosol

Arthur J. Sedlacek III[a], Timothy B. Onasch[b,c] [ID], Leonid Nichman[c] [ID], Ernie R. Lewis[a], Paul Davidovits[c], Andrew Freedman[b] [ID], and Leah Williams[b]

[a]Environmental and Climate Sciences Department, Brookhaven National Laboratory, Upton, New York, USA; [b]Aerodyne Research Inc., Billerica, Massachusetts, USA; [c]Department of Chemistry, Boston College, Chestnut Hill, Massachusetts, USA

Introduction

Black carbon (BC) in the atmosphere continues to be a focus of research because its light-absorptive properties put it second only to CO_2 as a warming agent of Earth's climate. Towards this end, the measurement of ambient BC has been aided greatly by the development of the Single Particle Soot Photometer (SP2)—an instrument that detects refractory black carbon (rBC) through laser-induced incandescence (Schwarz et al., 2006). Potential interference from other substances that can incandesce under 1064 nm illumination (e.g., some metals and minerals) is mitigated through the use of spectral bandpass filters that allow determination of the color temperature of incandescence to ensure that the SP2 remains highly selective to rBC. Here, we report on the detection of rBC that is produced through SP2 laser-induced charring (i.e., carbonization) of organic aerosols. Nigrosin and fulvic and humic acids—non-BC-containing materials—were used as a surrogates for light-absorbing organic aerosols. The color temperature of the detected particles originating from these charred organic aerosols is near that of carbon black, fullerene soot, and ethylene soot, indicating that the incandescent particles are composed of rBC. Failure to properly account for this heretofore unidentified artifact of the SP2 will lead to an overestimate of rBC loadings, which could, in turn, impact aerosol radiative forcing model predictions.

Methods

Aerosols were generated from deionized water-based stock solutions of nigrosin (Aldrich, 198285; NKbg74932; 4 mg/g) and carbon black (CAB-O-JET® 200 pigment; Cabot Corp; 110 mg/g) using a constant output atomizer (TSI; model 3076) and dried inline in a diffusion drier (Topas; model DDU 570/H). Nigrosin, a water-soluble, polyaniline-based black dye is often used in studies of atmospheric aerosol absorption as it possesses a broad, featureless absorption spectrum in the visible and near-IR (Bluvshtein et al., 2017; Hung et al., 2015) and dries to make spherical particles (Lack et al., 2006). Carbon black was used as BC reference material for comparison with nigrosin. Additional experiments were carried out using Suwannee River fulvic acid standard I (1S101F, IHSS) and Leonardite humic acid standard (1S104H, IHSS), fullerene soot (a calibration standard for the SP2 instrument; Gysel et al., 2011), and ethylene flame-generated soot.

Particles used in these experiments were selected by their mobility diameter (DMA, TSI model 3081) or the combination of mobility diameter and mass using a Centrifugal Particle Mass Analyzer (CPMA, Cambustion Ltd.). A mixing condensation particle counter (MCPC, BMI model 1710) was used to monitor particle number concentrations. A tube oven (Lindberg/Blue M) was used to heat the particles. The Single Particle Soot Photometer (SP2; Droplet Measurement Technologies; revision D) was used to detect rBC. The SP2 also allowed determination of the incandescence onset time, $\Delta\tau$—the
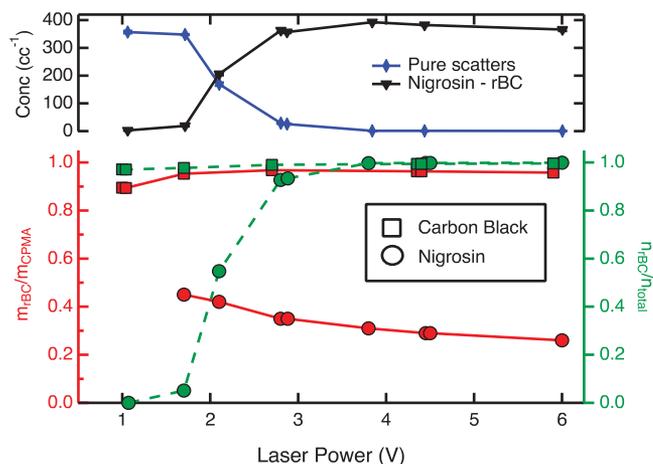
Figure 1. Upper panel: the number of detected rBC (downward triangles) and pure scattering (diamonds) particles as a function of SP2 laser power for nigrosin. Lower panel, left axis: ratio of SP2-derived rBC particle mass to original particle mass selected by the CPMA as a function of laser power for nigrosin (red circles) and carbon black (red squares); right axis: number fraction of BC particles to total number of particles detected by the SP2 for nigrosin (green circles) and carbon black (green squares) as a function of laser power.

time between the peak in incandescence signal and the peak of the scattering signal. This approach is similar to the lagtime methodology sometimes used in SP2 analysis of coated rBC particles (Sedlacek III et al., 2015). To minimize the effects of particle size on SP2 detection efficiency (Schwarz et al., 2010), 400 nm mobility diameter particles (e.g., 30 fg for nigrosin and 19 fg for carbon black) were studied exclusively, and the particle number concentrations were kept low ($<1000\,\mathrm{cm}^{-3}$) to minimize particle coincidence in the instrument.

Results and discussion

The charring of nigrosin particles is illustrated in Figure 1. The number concentrations of SP2-detected rBC and pure scattering particles as a function of SP2 laser power, shown in the upper panel, exhibit two striking features. First, incandescing particles are detected for the nigrosin aerosol. Second, the number concentrations of incandescing and non-incandescing nigrosin particles are inversely dependent on laser power, with more scattering particles being detected at lower laser powers, and more incandescing particles being detected at higher laser powers, although the sum was constant. This behavior indicates that the detected rBC originates from nigrosin despite the fact that nigrosin is a polyaniline-based black dye that does not contain rBC.

The ratio of rBC particle mass derived from the SP2 (under the assumption that the SP2 incandescence-to-mass ratio is the same for rBC derived from laser charring as it is for carbon black) to the original particle mass selected by the CPMA (left axis), which

characterizes the efficiency of charring of nigrosin particles by the SP2 laser, is shown in the lower panel of Figure 1. This value is 25–45% (depending on laser power) for nigrosin, but near unity for carbon black. This latter value is expected as the SP2 laser power fluence exceeds the ability of an individual particle to dissipate the absorbed energy, and indicates that the lowest laser power used in these experiments is sufficient to detect rBC with high efficiency. The absence of a mass ratio for nigrosin at the lowest laser power demonstrates that negligible rBC was generated at this laser power. The rBC number fraction as a function of SP2 laser power, shown on the right axis, demonstrates that carbon black particles are almost entirely detected as incandescing particles, independent of laser power, while the fraction of incandescing particles derived from nigrosin is strongly dependent on the laser power.

The behavior exhibited by nigrosin under varying laser power suggests that nigrosin is charring, thereby producing the rBC detected by the SP2. Nigrosin possesses a broad absorption spectrum that spans into the near-IR, with an imaginary component of refractive index at 1064 nm estimated to be 0.07 based on Bluvshtein et al. (2017) and Hung et al. (2015). The proposed explanation for this behavior is that nigrosin molecules absorb 1064 nm laser light, heating the particle sufficiently that chemical reactions result in charring of a fraction of the nigrosin, with the formed rBC material continuing to heat in the SP2 laser until incandescence. The trend of a decreasing fraction of the original nigrosin mass charring with increasing laser power (Figure 1), and an observed decrease in
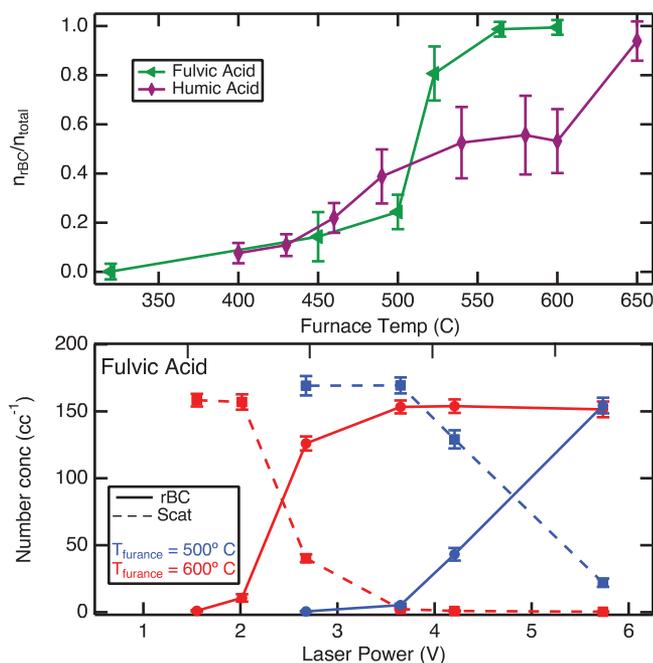
Figure 2. Upper panel: the ratio of the number fraction of rBC particles to total number of particles detected by the SP2 for fulvic and humic acids as a function of tube furnace temperature at a SP2 laser power of 4.3 V. Lower panel: number concentration of rBC and scattering fulvic acid particles at oven temperatures of 500 and 600 °C as a function of the SP2 laser power. Similar behavior was observed for humic acid (not shown).

incandescence onset times with increasing laser power (not shown) suggest competing rates between the charring reactions and the heating of the charred rBC to incandescence, effectively shutting off further charring.

The observation of rBC from nigrosin suggests that if an organic particle can absorb light at 1064 nm, it can be induced to produce rBC under sufficiently high SP2 laser power. To test this hypothesis, a set of experiments was conducted using aerosolized fulvic acid and humic acid dry particles—surrogates for HULIS—and examining the production of rBC from these particles as a function of tube furnace temperature and SP2 laser power. A flow of aerosolized particles was passed through a stainless steel (309S) tubing inside the furnace. The number fraction of rBC produced as a function of oven temperature for a constant SP2 laser power (4.3 V) for both HULIS materials is shown in the upper panel of Figure 2. At the lowest furnace temperatures examined, negligible amounts of rBC were detected, but as the temperature increased there was concomitant increase in the rBC number fraction, and at sufficiently high furnace temperature, all particles were detected by SP2 as rBC.

The observations in Figure 2 suggests that the initially near-IR transparent fulvic and humic acid particles at room temperature undergo chemical transformations as the furnace temperature is increased, creating new near-

IR absorption transitions that enable SP2-induced charring. To explore this idea further, we examined the rBC production for fulvic acid as a function of laser power at two furnace temperatures: 500 and 600 °C (Figure 2, bottom panel). As the furnace temperature was increased from 500 to 600 °C, the laser power necessary to induce fulvic acid charring decreased by approximately half. This dependence on furnace temperature suggests that fulvic acid becomes more absorbing at higher furnace temperatures. Similar behavior was exhibited by humic acid (not shown). It is interesting to note that the crossover laser power (~2.5 V) where more rBC is detected than pure scatters at 600 °C is similar to the crossover point observed for nigrosin (~2.1 V), suggesting a similar magnitude for the imaginary component of the refractive index for the modified fulvic acid.

While the furnace temperatures necessary to induce the near-IR absorption transitions for fulvic acid and humic acid are higher than those typically used for thermal denuders, individual organic substances are expected to exhibit a range of properties, and thus could exhibit a similar increase in absorption at typical denuder temperatures. The results presented here indicate that SP2-induced charring of organic aerosol can occur under some operating conditions and thus could bias the true rBC loading values and, in turn, subsequent conclusions that would be drawn using such data. This is clearly an
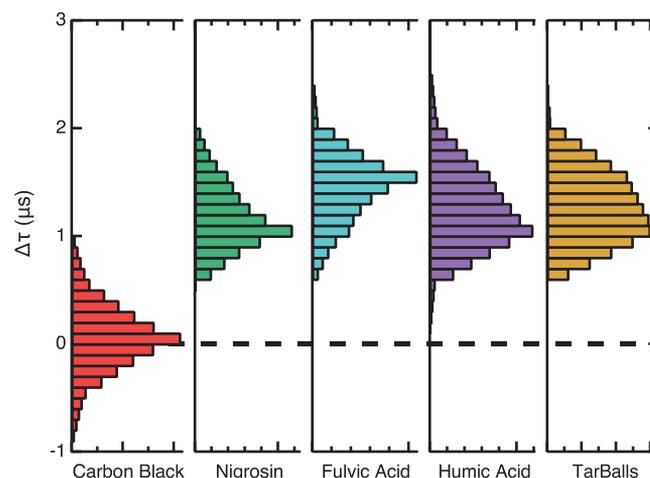
Figure 3. Histograms of the incandescence onset times for carbon black (red), nigrosin (green), fulvic acid (aqua), humic acid (purple), and tar balls (beige).

area that needs to be more systematically explored to better bound this impact on ambient measurements of rBC.

The dependence of the incandescence detection efficiency of absorbing organic aerosol on SP2 laser power suggests a method for distinguishing between preexisting rBC and laser-induced charring. As all particles containing rBC will be detected at all laser powers above a minimum threshold, any further increase in the number or per-particle mass of SP2-detected rBC particles with increasing laser power must result from non-rBC particulate matter that absorbs radiation at the SP2 laser wavelength and chars as a result. Additionally, measurement of the increase in the number or mass of per-particle rBC with increasing laser power could provide an estimate of the imaginary component of the refractive index of near-IR absorbing species relative to a standard, such as nigrosin.

The particle types discussed thus far are idealized surrogates and leave the question as to the significance of these results towards atmospherically-relevant aerosols. Light-absorbing organic aerosols, commonly referred to as brown carbon (BrC) for their tendency to absorb predominantly in the mid- to short-wave spectrum, are recognized as another important direct radiative forcing agent (Andreae & Gelencsér 2006; Chen and Bond 2010; Feng, Ramanathan, and Kotamarthi 2013). However, there is at least one class of atmospherically-relevant BrC particles that absorbs at longer wavelengths: Tar balls (TBs), an abundant type of carbonaceous particle that appears to be the near exclusive byproduct of some types of biofuel combustion/pyrolysis and wildfires (Pósfai et al., 2004; Adachi and Buseck 2011; Sedlacek III et al., 2018).

Hoffer et al. (2017) reported that laboratory generated tar balls exhibit appreciable absorption (imaginary component of refractive index, m_I, equal to 0.2i at 550 nm) extending into the near-IR; however, recent field observations suggest ambient tar balls may be less absorbing ($m_I \sim 0.02i$ at 532 nm) than laboratory tar balls (Sedlacek III et al., 2018). While it is unknown what fraction of ambient particles absorb 1064 nm wavelength light, we report results that suggest that it is likely that ambient tar balls exhibit some degree of charring in the SP2.

In a separate series of experiments to examine the refractory character of TB particles, we pyrolyzed pine needles and twigs using the synthesis procedure described by Tóth et al. (2014) and sampled these laboratory-generated, polydisperse particles with the SP2. Microscopy analysis confirmed the production of TBs via this method, and incandescence and color temperature signals observed by the SP2 indicate the presence of rBC ($\sim$9% mass loading ratio). This rBC resulted either from charring of OA at 600 °C (the pyrolysis temperature) or from SP2-induced charring through near-IR light absorption as observed with nigrosin and fulvic and humic acids; the mechanism could be unambiguously distinguished as the laser power was not varied during these experiments. We examined the incandescence onset time as a measure of the time necessary for the SP2 laser to induce charring by the light absorbing OA before incandescence. Histograms of these times for carbon black, nigrosin, fulvic acid, humic acid, and laboratory-generated tar balls, shown in Figure 3, clearly demonstrate that there are two types of behavior: the latter four species all exhibit similar nonzero values near 1.2 µs, whereas

that for carbon black is centered about 0 µs. The similarity of the incandescent onset time observed for TBs with that for particle types that undergo SP2-induced charring suggests that production of observed rBC in TBs occurred through a similar mechanism. This result also suggests that SP2 measurements in biofuel/biomass plumes containing TBs could result in overestimation of the rBC loadings.

Finally, it is interesting to consider the potential impact of these findings for those measurement schemes that employ thermal denuders as a method of removing semivolatile organic aerosols ("coatings") associated with rBC. As has been documented elsewhere (Swanson and Kittelson 2010; Yu, Xu, and Yang 2002), charring of organic aerosol can readily occur during the thermal denuding process. To be clear on a subtle but important point, the charring discussed in the literature is that directly brought about by the particle heating in the thermal denuder and is to be distinguished from the SP2-induced charring by 1064 nm light absorbing organic aerosol. Our results provide a method for distinguishing these different charring mechanisms. While the efficiency of charring via this method depends upon temperature, rate of heating, composition, and amount of material, overestimation of rBC would occur if the charring efficiency was non-negligible.

In summary, we have demonstrated that production of rBC can occur by charring of light-absorbing organic particles that did not originally contain rBC. This production of rBC has been observed for particle containing substances that absorb at the SP2 laser wavelength as a fundamental property of the substance (nigrosin), and for particles containing substances that are induced to absorb at the SP2 laser wavelength through thermally-catalyzed chemical reactions such as may occur in a thermal denuder (fulvic acid and humic acid). If examining a mixture of aerosol types (e.g., ambient), this behavior could result in an overestimate of rBC, and thus misapportionment of BC and BrC, with implications for models attempting to simulate radiative forcing from biomass burning. The production of rBC from BrC could have been a factor in the BC/BrC correlation reported by Saleh et al. (2014).

Acknowledgments

Funding

ORCID

Timothy B. Onasch ⓘ http://orcid.org/0000-0001-7796-7840
Leonid Nichman ⓘ http://orcid.org/0000-0003-3923-1589
Andrew Freedman ⓘ http://orcid.org/0000-0002-5598-6626

References

Adachi, K., and P. R. Buseck. 2011. Atmospheric tar balls from biomass burning in Mexico. *J. Geophys. Res.-Atmos.* 116:D05204. doi:10.1029/2010JD015102.

Andreae, M. O., and A. Gelencsér. 2006. Black carbon or brown carbon? the nature of light-absorbing carbonaceous aerosols. *Atmos. Chem. Phys.* 6(10):3131–48. doi:10.5194/acp-6-3131-2006.

Bluvshtein, N., J. M. Flores, Q. He, E. Segre, L. Segev, N. Hong, A. Donohue, J. N. Hilfiker, and Y. Rudich. 2017. Calibration of a multi-pass photoacoustic spectrometer cell using light-absorbing aerosols. *Atmos. Meas. Tech.* 10(3):1203–13. doi:10.5194/amt-10-1203-2017.

Chen, Y., and T. C. Bond. 2010. Light absorption by organic carbon from wood combustion. *Atmos. Chem. Phys.* 10(4):1773–87. doi:10.5194/acp-10-1773-2010.

Feng, Y., V. Ramanathan, and V. R. Kotamarthi. 2013. Brown carbon: A significant atmospheric absorber of solar radiation? *Atmos. Chem. Phys.* 13(17):8607–21. doi:10.5194/acp-13-8607-2013.

Gysel, M., M. Laborde, J. S. Olfert, R. Subramanian, and A. J. Gröhn. 2011. Effective density of Aquadag and fullerene soot black carbon reference materials used for SP2 calibration. *Atmos. Meas. Tech.* 4(12):2851–58. doi:10.5194/amt-4-2851-2011.

Hoffer, A., A. Tóth, M. Pósfai, C. E. Chung, and A. Gelencsér. 2017. Brown carbon absorption in the red and near infrared spectral region. *Atmos. Meas. Tech.* 10(6):2353–59. doi:10.5194/amt-10-2353-2017.

Hung, C.-H., T.-C. Chou, C.-K. Hsu, and S.-H. Tseng. 2015. Broadband absorption and reduced scattering spectra of in-vivo skin can be noninvasively determined using δ-P1 approximation based spectral analysis. *Biomed. Opt. Express* 6(2):443. doi:10.1364/BOE.6.000443.

Lack, D. A., E. R. Lovejoy, T. Baynard, A. Pettersson, and A. R. Ravishankara. 2006. Aerosol absorption measurement using photoacoustic spectroscopy: Sensitivity, calibration, and uncertainty developments. *Aerosol Sci. Technol.* 40(9):697–708. doi:10.1080/02786820600803917.

Pósfai, M., A. Gelencsér, R. Simonics, K. Arató, J. Li, P. V. Hobbs, and P. R. Buseck. 2004. Atmospheric tar balls: Particles from biomass and biofuel burning. *J. Geophys. Res.* 109:D06213. doi:10.1029/2003JD004169.

Saleh, R., E. S. Robinson, D. S. Tkacik, A. T. Ahern, S. Liu, A. C. Aiken, R. C. Sullivan, A. A. Presto, M. K. Dubey, R. J. Yokelson, et al. 2014. Brownness of organics in aerosols from biomass burning linked to their black carbon content. *Nat. Geosci.* 7(9):647–50. doi:10.1038/ngeo2220.

Schwarz, J. P., R. S. Gao, D. W. Fahey, D. S. Thomson, L. A. Watts, J. C. Wilson, J. M. Reeves, M. Darbeheshti, D. G. Baumgardner, G. L. Kok, et al. 2006. Single-particle measurements of midlatitude black carbon and light-scattering aerosols from the boundary layer to the lower stratosphere. *J. Geophysical Res.* 111:D16207. doi:10.1029/2006JD007076.

Schwarz, J. P., J. R. Spackman, R. S. Gao, A. E. Perring, E. Cross, T. B. Onasch, A. Ahern, W. Wrobel, P. Davidovits, J. Olfert, et al. 2010. The detection efficiency of the single particle soot photometer. *Aerosol Sci. Technol.* 44(8):612–28. doi:10.1080/02786826.2010.481298.

Sedlacek III, A. J., P. R. Buseck, K. Adachi, T. B. Onasch, S. R. Springston, and L. I. Kleinman. 2018. Formation and evolution of tar balls from northwestern US wildfires. *Atmos. Chem. Phys.* 18(15):11289–301. doi:10.5194/acp-18-11289-2018.

Sedlacek III, A. J., E. R. Lewis, T. B. Onasch, A. T. Lambe, and P. Davidovits. 2015. Investigation of refractory black carbon-containing particle morphologies using the single-particle soot photometer (SP2). *Aerosol Sci. Technol.* 49(10):872–85. doi:10.1080/02786826.2015.1074978.

Swanson, J., and D. Kittelson. 2010. Evaluation of thermal denuder and catalytic stripper methods for solid particle measurements. *J. Aerosol Sci.* 41(12):1113–22. doi:10.1016/j.jaerosci.2010.09.003.

Tóth, A., A. Hoffer, I. Nyirő-Kósa, M. Pósfai, and A. Gelencsér. 2014. Atmospheric tar balls: Aged primary droplets from biomass burning? *Atmos. Chem. Phys.* 14(13):6669–75. doi:10.5194/acp-14-6669-2014.

Yu, J. Z., J. Xu, and H. Yang. 2002. Charring characteristics of atmospheric organic particulate matter in thermal analysis. *Environ. Sci. Technol* 36(4):754–61. doi:10.1021/es015540.